

Effect of hydrogen molecules on the electronic transport through atomic-sized metallic junctions in the superconducting state

P. Makk, Sz. Csonka, and A. Halbritter

Department of Physics, Budapest University of Technology and Economics and Condensed Matter Research Group of the Hungarian Academy of Sciences, 1111 Budapest, Budafoki ut 8, Hungary

(Received 6 March 2008; revised manuscript received 3 June 2008; published 15 July 2008)

In this paper the interaction of hydrogen molecules with atomic-sized superconducting nanojunctions is studied. It is demonstrated by conductance histogram measurements that the superconductors niobium, tantalum, and aluminum show a strong interaction with hydrogen, whereas for lead a slight interaction is observed and for tin and indium no significant interaction is detectable. For Nb, Ta, and Pb the subgap method is applied to determine the transmission eigenvalues of the nanojunctions in hydrogen environment. It is shown that the behavior of Nb and Ta nanojunctions is strongly modified by hydrogen molecules as reflected by the pronounced changes in the conductance histogram, the appearance of extremely long conductance traces, and the observation of negative differential conductance phenomenon in the dI/dV curve. Surprisingly the transport properties based on the measured transmission eigenvalues are similar to those of pure junctions. Our results imply that in Nb and Ta the interaction with hydrogen causes a plastic, ductile behavior and the formation of long nanoscale necks, but no well-defined single-molecule contacts are formed, and the transport properties are still dominated by Nb and Ta.

DOI: [10.1103/PhysRevB.78.045414](https://doi.org/10.1103/PhysRevB.78.045414)

PACS number(s): 74.78.Na, 73.63.Rt, 81.07.Nb, 85.65.+h

I. INTRODUCTION

The future aim of building functional single-molecule electronic devices necessitates the development of reliable characterization techniques of molecular nanojunctions. In many cases the direct microscopic imaging of the junction is not possible; thus all the information about the molecular device must be extracted from its electronic properties.^{1-8,10,11} The conduction properties of the device can be characterized by the so-called mesoscopic PIN code,¹ the set of the transmission eigenvalues of the junction. According to the Landauer formula, the linear conductance of the junction is proportional to the sum of the transmission eigenvalues, $G=2e^2/h\sum\tau_i$, where $G_0=2e^2/h$ is the quantum conductance unit. For the determination of the individual transmission eigenvalues, the measurement of further quantities is required. Conductance fluctuation and shot-noise measurements provide an additional independent combination of the mesoscopic PIN code; $\sum\tau_i(1-\tau_i^2)$ and $\sum\tau_i(1-\tau_i)$, respectively, can be determined.^{12,13} These methods were successfully applied in the study of molecular nanojunctions,^{2,3,6} showing that hydrogen forms a perfectly transmitting single-molecule bridge between platinum electrodes,^{2,3} whereas for the isoelectronic metal palladium no similar structure is formed.⁶ However, for a junction with arbitrary conductance and a larger number of conductance channels, the conductance fluctuation and shot-noise measurements are not efficient.

By placing the junction between superconducting electrodes and measuring the nonlinear subgap features in the current-voltage characteristics, principally all the transmission eigenvalues can be determined. This method was successfully used in the study of single-atom junctions of Nb, Pb, and Al, demonstrating that even for a junction with five or six conductance channels the transmission eigenvalues can be determined with high precision.¹⁴⁻¹⁷ With the use of

proximity effect, the subgap method can even be extended for nonsuperconducting materials, as shown by the subgap measurements on gold nanojunctions.^{18,19} According to our knowledge, studies on molecular nanojunctions applying the superconducting subgap method have not yet been reported.

Besides the study of the mesoscopic PIN code and the corresponding elastic transmission properties of the junction, a fingerprint of the inelastic excitations of the molecular device can be given by point-contact spectroscopy and inelastic-electron-tunneling spectroscopy measurements. The excitation of the vibrational modes of the molecular device,⁷ or the excitation of the molecule to other configurations with different binding energy,⁸ is reflected by steplike or even peaklike structures in the differential conductance, $dI/dV(V)$, characteristics. As the subgap features appear below the superconducting gap on the millivolt or even submillivolt scale, whereas the inelastic excitations are typically observed in the range of 30–100 mV, from a single $I-V$ curve measurement both features can be recorded. Therefore, the break junction method with superconducting electrodes provides a powerful tool for the study of molecular nanojunctions: Besides the fine tuning of the electrode separation, both the elastic transmission eigenvalues of the junctions can be determined and the inelastic excitations of the junction can be studied. All these together provide an outstanding amount of information about the studied molecular nanostructures.

In this paper we study the behavior of superconducting atomic-sized nanojunctions in an interaction with the simplest molecule, hydrogen. As superconducting electrodes, Nb, Ta, Al, Pb, Sn, and In samples were used. For all these materials, the interaction is investigated by the conductance histogram technique; for Nb, Ta, and Pb the subgap curves of the molecular nanojunctions are also studied. The $I-V$ characteristics of the molecular junctions show clear-cut subgap features, from which the transmission eigenvalues can be extracted with high precision.

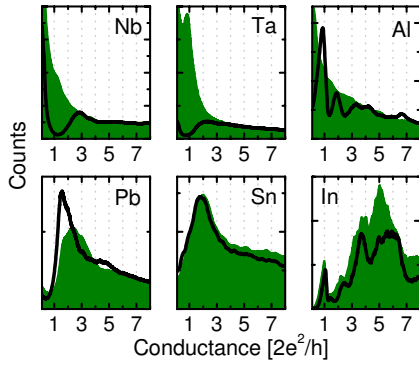


FIG. 1. (Color online) Conductance histograms of Nb, Ta, Al, Pb, Sn, and In junctions in high vacuum (line graphs) and in hydrogen environment (area graphs). The histograms were recorded at $T=4.2$ K and $V=10$ mV (Ref. 9). All the histograms are normalized to the precise number of the included traces (4000–8000).

II. EXPERIMENTAL METHOD

Our experiments were performed by following the mechanically controllable break junction (MCBJ) technique at liquid-helium temperature ($T=2.2$ – 4.2 K). The atomic-sized nanojunctions were created under cryogenic vacuum by breaking high-purity wires. The hydrogen molecules were admitted to the sample space through a solenoid valve of a mass flow controller from a container of high-purity hydrogen with reduced pressure (~ 10 mbar). For the removal of contaminants, a liquid-nitrogen cold trap was used. By applying short pulses of 100 ms on the solenoid valve, doses of ~ 0.1 μmol H_2 could be admitted to the sample holder. The molecules were directed to the close vicinity of the junction in the cryogenic part of the setup through a capillary tube. The measurements were performed in a voltage biased setup. In the I - V curve measurements, special attention was taken to protect the sample from noise pickups, which would smear out the nonlinear features. For the reduction of the noise level, the input voltage signal was attenuated by a 1:100 divider. Conventional RC low-pass filters with cut-off frequency of 100 kHz were placed close to the junction to reduce high-frequency pickups. According to the width of the peaks in the $dI/dV(V)$ curves of superconducting Nb, Ta, and Pb tunnel junctions, the noise level was lower than 80 μV .

III. CONDUCTANCE HISTOGRAMS AND INDIVIDUAL CONDUCTANCE TRACES

Figure 1 shows the conductance histograms of Nb, Ta, Al, Pb, Sn, and In junctions both in high vacuum and in hydrogen environment. The histograms are constructed from a large number of conductance vs electrode separation traces recorded during the opening of the junctions. In pure environment the d metals Nb and Ta and the p metals Pb and Sn exhibit a single broad peak corresponding to single-atom junctions, whereas the p metal Al shows more well-defined peaks. All these results agree with previous observations.¹ Indium, for which former measurements are not known to us, shows a rather unique histogram: A sharp peak is observed at

the conductance quantum unit, and further features are seen at higher conductance values.

In hydrogen environment the histograms of Pb, Sn, and In show a similar shape as that in high vacuum. For lead the peak becomes broader and shows a significant shift toward higher values, whereas tin does not show any change. For indium the $1G_0$ peak is reproduced, and the change at higher conductance values is within the scatter of the pure histograms from sample to sample. In contrast for Nb, Ta, and Al the addition of hydrogen has a very strong influence on the histograms. In every case a rather featureless distribution is observed, demonstrating the appearance of a large number of different hydrogen-related configurations. In Nb usually a small shoulder near the quantum conductance unit is superimposed onto the featureless histogram. In Ta even a small peak at $1G_0$ can be seen after the admission of hydrogen, which disappears by time, as already reported in Ref. 11. It is noted that all the hydrogen-related features disappear if the histograms are recorded at large bias voltage ($V \approx 300$ – 400 mV), as the hydrogen is desorbed due to the local heating of the junction.⁵

As the histograms are normalized to the number of traces included, the weights in pure and hydrogen environments can be directly compared. Accordingly, at higher conductance values, where the effect of hydrogen is negligible, the two histograms fall onto each other. For aluminum the overall weights of the two histograms are similar; only the characteristic peaks of aluminum are smoothed out in the hydrogen-affected histogram. In Nb and Ta a remarkable feature is observed: Above the conductance of the pure single-atom contacts ($G \approx 2.3G_0$), the two histograms are almost the same, but below that value the pure histogram shows a minimum, whereas in the hydrogen-affected case a huge weight is observed.

We have found that the strong interaction of Nb, Ta, and Al with hydrogen is not only statistically detectable by conductance histograms, but it is also clearly visible on individual conductance traces. The red curves in Fig. 2 show typical conductance traces of pure Nb, Ta, and Al. After forming a single-atom junction, a sudden jump to the tunneling region is observed during the opening of the junction. In contrast the conductance traces in hydrogen environment show various different conductance values with a lot of jumps. The difference is remarkable; just by looking at a single conductance trace, the presence of hydrogen can be detected. In the case of Nb and Ta, it is clearly visible that the hydrogen-affected traces are significantly longer than the pure traces. Surprisingly, this kind of traces is not observed only during the rupture of the junction, but the same behavior is seen when the electrodes are pushed together. In the case of aluminum, the characteristic positive slope of the plateaus is preserved in hydrogen environment; just several smaller jumps are observed instead of the few larger jumps in high vacuum. For Pb, Sn, and In the characteristic shape of the individual conductance traces did not change upon the addition of hydrogen, as expected.

The effect of hydrogen can be further studied by investigating the length of the conductance traces. As the plateaus' length histograms did not show any distinct feature (e.g., chain formation^{4,20}), we characterize the length of the traces

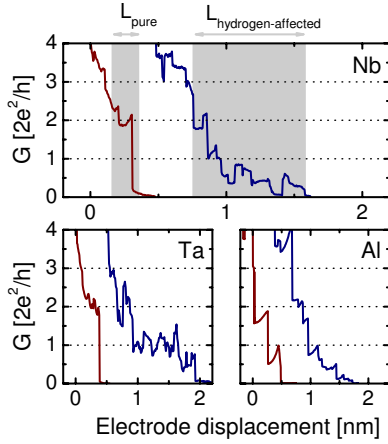


FIG. 2. (Color online) Typical conductance traces of Nb, Ta, and Al junctions in high vacuum (left, red curves) and in hydrogen environment (right, blue curves) recorded during the opening of the junctions. The gray region in the top panel demonstrates the length required for the disconnection of the junction (see text).

with a single number, the average distance between the position of the single-atom peak in the pure histogram ($2.3G_0$ for Nb and Ta and $0.85G_0$ for Al) and $0.1G_0$ during the opening of the junction (the definition of this length is illustrated in the upper panel of Fig. 2). According to calibration measurements based on the exponential variation of the tunnel current, in pure environment this average length is approximately 1 Å for all the three metals. In hydrogen environment the traces of aluminum junctions are slightly longer: The above defined average length is 1.4 times larger than that of pure junctions. In niobium and tantalum, a huge increase is observed; the hydrogen-affected traces are *six to nine times longer* than the pure ones. A similar increase is also observed if the length is measured during the closing of the junctions.

IV. SUBGAP ANALYSIS

Figure 3 shows the results of an I - V curve measurement on a $G \approx 1G_0$ Nb junction in hydrogen environment. Panel (a) shows the differential conductance, dI/dV , in a wide voltage window. The curve shows a negative differential conductance peak at $V=40$ mV and a large noise at higher voltages. Both features are characteristic of molecular nanojunctions and cannot be seen in pure environment. The negative differential conductance peak is related to the scattering on a two-level system formed by the molecular junction, but the more precise microscopic background of the phenomenon is still debated.^{8,10} The observation of a shoulder at the quantum conductance unit in the histogram of niobium-hydrogen junctions, together with the appearance of a peaklike structure close to the previously observed vibrational energy in Pt- H_2 single-channel molecular bridges, could imply the formation of a hydrogen molecular bridge between the niobium electrodes similar to that in the Pt- H_2 system.^{2,7} This hypothesis can be tested by zooming in on the superconducting features in the middle of the I - V curve. Figure 3(b) shows the differential conductance within the gap region exhibiting dis-

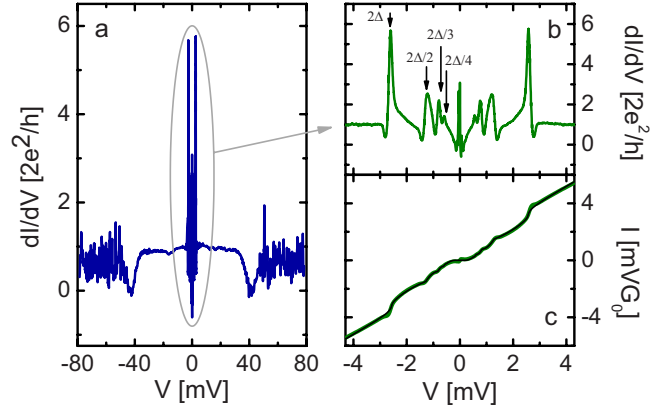


FIG. 3. (Color online) I - V curve measurement on a hydrogen-affected Nb junction with $G \approx 1G_0$. (a) The differential conductance in a wide voltage window, showing negative differential conductance phenomenon and a large conductance noise at higher voltages. (b) Differential conductance in the superconducting gap region. (c) I - V curve in the superconducting gap region and the best theoretical fit corresponding to the set of channel transmissions $\{0.70, 0.14, 0.08, 0.05, 0.04\}$.

tinct peaks at the fractional values of the gap due to multiple Andreev reflections.^{14,15} Figure 3(c) shows the I - V curve itself, which is fitted to the theory of multiple Andreev reflections.¹⁶ The fitting shows that the junction has five open channels, and the corresponding transmission probabilities are $\{0.70, 0.14, 0.08, 0.05, 0.04\}$. This result clearly shows that no single-channel hydrogen molecular bridge is formed. Figure 4 shows further examples of subgap curves in niobium-hydrogen junctions with $G \approx 1G_0$. It is seen that occasionally subgap curves with a single, perfectly transmitting conductance channel are indeed observed, but these curves were rather rare, and occasionally similar curves were also observed in pure Nb junctions. In the majority of the cases, the second conductance channel also gives a significant contribution. We note that in our measurements we did not observe clear vibrational spectra like that in the Pt- H_2 system.^{2,7} In hydrogen environment rather huge peaklike structures and/or large noise of the conductance at higher bias voltage were seen, which are both demonstrated in Fig. 3.

Taking advantage of the fact that with the subgap method the complete mesoscopic PIN code of the junction can be

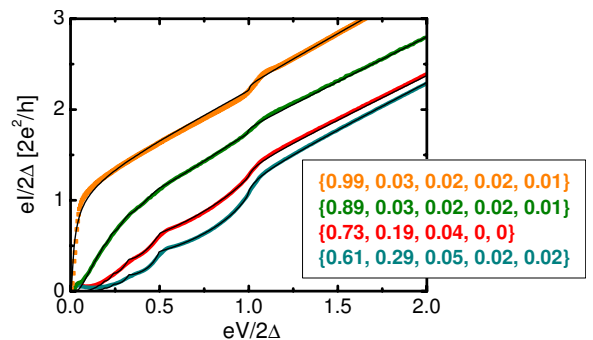


FIG. 4. (Color online) Subgap structure measurements on four different niobium junctions in hydrogen environment with $G \approx 1G_0$. The set of transmission eigenvalues corresponding to the best fits (thin black lines) are also indicated on the figure.

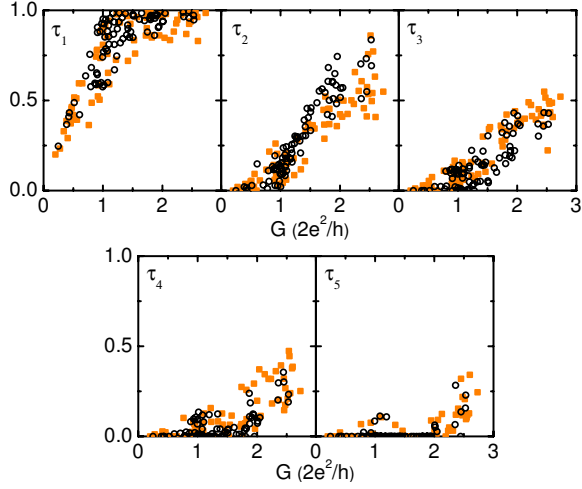


FIG. 5. (Color online) Transmission probabilities of a large amount of independent Ta contacts in high vacuum (orange squares) and in hydrogen environment (black circles) as a function of conductance.

determined at an arbitrary point of the conductance trace, we have performed a large number of subgap measurements in a wide conductance interval of $0.1G_0-3G_0$ for both pure and hydrogen-affected Nb, Ta, and Pb junctions. Our measurements show the strange result that in the whole conductance interval, no statistical difference can be pointed out between the channel distributions of the pure and hydrogen-affected junctions. This result is demonstrated for Ta junctions in Fig. 5. The five panels show the distribution of the transmission probabilities for a large number of independent configurations both in pure and hydrogen environments. It is clear that the opening of the conductance channels follow the same tendency for pure and hydrogen-affected junctions; the measured points fall onto each other within the scattering of the data. The same behavior was observed for Nb and Pb junctions

as well, for which the results are demonstrated in Table I, showing the mean value and the standard deviation of the channel transmissions at some characteristic conductance values. For Nb these values were chosen to be $0.3G_0$, corresponding to a point from the tail of the hydrogen-affected histogram with a large weight; $1G_0$, corresponding to the shoulder in the hydrogen-affected histogram; and $2.3G_0$, corresponding to the peak due to single-atom contacts in the pure histogram. For Pb the results for $1.5G_0$ and $2.2G_0$ are presented, corresponding to the peak positions in the pure and hydrogen-affected histograms, respectively. For comparison the results for Ta junctions with $G=1G_0$, corresponding to the peak in the hydrogen-affected histogram, are also shown. It is seen that at each conductance value, the mean value of all the transmission coefficients for pure and hydrogen-affected junctions are the same well within the standard deviation of the data. In contrast it is worth noting that Nb and Ta have very similar electronic structures, but still the distribution of the channel transmissions of pure Nb and Ta junctions are well distinguishable from each other (see Table I), which demonstrates the strength of the subgap method.

V. SUMMARY AND DISCUSSION OF THE RESULTS

Our measurements have shown that in Nb, Ta, and Al junctions, the conductance histograms are strongly reshaped due to the interaction with hydrogen; in Pb some effect of hydrogen is observed, whereas in Sn and In no significant change is observed.

In Al junctions the results imply that hydrogen stabilizes various arrangements with slightly different conductance values, and so the histogram is smoothed out and the individual traces show several smaller steps. The overall weight of the histogram and length of the traces do not change considerably, and the characteristic shape of the plateaus with posi-

TABLE I. The mean value and the standard deviation of the transmission eigenvalues at some characteristic conductance values of Nb, Ta, and Pb junctions both in high vacuum and in hydrogen environment. The indicated conductance values were adjusted with an accuracy of $0.03G_0$, and at each conductance value the subgap curves were recorded on 30 independent junctions.

	$G=0.3G_0$		$G=1G_0$		$G=2.3G_0$	
	Nb	Nb+H ₂	Nb	Nb+H ₂	Nb	Nb+H ₂
τ_1	0.27 ± 0.03	0.27 ± 0.03	0.71 ± 0.14	0.7 ± 0.13	0.93 ± 0.07	0.89 ± 0.08
τ_2	0.02 ± 0.01	0.02 ± 0.01	0.13 ± 0.08	0.17 ± 0.09	0.62 ± 0.13	0.55 ± 0.09
τ_3	0.01 ± 0.01	0.01 ± 0.01	0.08 ± 0.05	0.06 ± 0.03	0.42 ± 0.09	0.43 ± 0.11
τ_4			0.05 ± 0.03	0.04 ± 0.03	0.17 ± 0.09	0.22 ± 0.10
τ_5			0.03 ± 0.03	0.03 ± 0.03	0.16 ± 0.08	0.21 ± 0.08
	$G=1.5G_0$		$G=2.2G_0$		$G=1G_0$	
	Pb	Pb+H ₂	Pb	Pb+H ₂	Ta	Ta+H ₂
τ_1	0.90 ± 0.07	0.87 ± 0.07	0.95 ± 0.05	0.96 ± 0.04	0.81 ± 0.13	0.79 ± 0.16
τ_2	0.33 ± 0.07	0.34 ± 0.07	0.67 ± 0.07	0.66 ± 0.07	0.08 ± 0.06	0.11 ± 0.05
τ_3	0.23 ± 0.05	0.24 ± 0.05	0.34 ± 0.07	0.33 ± 0.06	0.07 ± 0.05	0.06 ± 0.06
τ_4	0.04 ± 0.05	0.05 ± 0.05	0.24 ± 0.06	0.25 ± 0.06	0.04 ± 0.02	0.04 ± 0.04
τ_5						

tive slope is also preserved. For the subgap analysis of aluminum-hydrogen junctions, subkelvin temperatures would be required, which is not available in our setup.

In Pb junctions the subgap analysis shows that the transmission probabilities in hydrogen environment are indistinguishable from those of pure junctions. This, together with the slight changes in the histogram, implies that the interaction of lead with hydrogen is weak.

Niobium and tantalum junctions show very similar behaviors, which is not surprising, as Nb is placed above Ta in the Periodic Table. Both metals show strong interaction with hydrogen; in H_2 environment a rather featureless histogram is observed, in which at low conductance values a huge weight grows compared to the pure histograms. For both metals some features can be seen close to the quantum conductance unit; in Nb, occasionally a shoulder is seen in the hydrogen-affected histogram, whereas in Ta even a peak can grow at $1G_0$, which disappears by time. The strong interaction with hydrogen is evident from individual conductance traces; instead of the sudden jump to tunneling, extremely long traces with a lot of jumps are observed. The length analysis shows that in hydrogen the average length to break a single-atom contact is six to nine times larger than that in high vacuum. This feature indicates a completely different mechanical behavior of hydrogen-affected Nb and Ta junctions. As no periodic peaks are observed in the plateaus' length histogram and the same extremely long traces are also observed during the closing of the junctions, the formation of atomic chains is not a plausible explanation for this strange phenomenon. Rather a very ductile behavior of the junction's neighborhood and the pulling of a long neck are expected. The subgap analysis of the hydrogen-affected junctions has shown that in spite of the growth of a shoulder or even a peak near the conductance quantum unit in the histograms of Nb and Ta and the frequent occurrence of peaklike structures in the differential conductance curves, the formation of a molecular hydrogen bridge with a single conductance channel is not observed in the large majority of the cases. Furthermore our results show that the mesoscopic PIN code of the hydrogen-affected junctions are the same as those of pure junctions in a wide conductance interval. This indicates that the transport properties are still dominated by Nb and Ta, though the mechanical behavior of the junctions is completely changed in hydrogen environment. All these results imply that a larger

number of molecules interacting with the metallic junction—and probably also being dissolved in the electrodes—cause a softening of the Nb-Nb bonds, resulting in a plastic, ductile behavior of the neighborhood of the junction and the pulling of a long, nanoscale neck, but no well-defined single-molecule contacts are formed.

VI. CONCLUSIONS

In conclusion, we have studied the effect of hydrogen molecules on the transport through atomic-sized junctions of the superconducting metals Nb, Ta, Al, Pb, Sn, and In. The histograms of Pb, Sn, and In junctions do not show any significant change in hydrogen environment, whereas for Al, Ta, and Nb the histograms are strongly reshaped due to the interaction with hydrogen. Nb and Ta junctions exhibit extremely long conductance traces in hydrogen environment. The distance for breaking a single-atom contact is six to nine times longer than for pure junctions, which implies the formation of long, nanoscale necks before the complete rupture of the junction. We have also applied the superconducting subgap method to determine the mesoscopic PIN code of molecular nanojunctions. Our measurements show the surprising result that the transmission probabilities of hydrogen-affected Nb and Ta junctions are the same as those of pure junctions, although all other experimental results (change in conductance histograms, extremely long conductance traces, and the appearance of negative differential conductance peaks in the dI/dV curve) indicate a very strong interaction with hydrogen. These results imply that the hydrogen abruptly changes the mechanical behavior of the junction, causing a plastic, ductile behavior and the formation of long nanoscale necks, but no well-defined single-molecule contacts are formed, and the transport properties are still dominated by Nb and Ta.

ACKNOWLEDGMENTS

This work was supported by Hungarian Research Funds (OTKA) F049330, NK72916. A.H. acknowledges the support of the Bolyai János Research Grant. The authors are grateful to G. Rubio-Bollinger for the multiple Andreev reflection fitting code.

¹N. Agrait, A. L. Yeyati, and J. M. van Ruitenbeek, *Phys. Rep.* **377**, 81 (2003).

²R. H. M. Smit, Y. Noat, C. Untiedt, N. D. Lang, M. C. van Hemert, and J. M. van Ruitenbeek, *Nature (London)* **419**, 906 (2002).

³D. Djukic and J. M. van Ruitenbeek, *Nano Lett.* **6**, 789 (2006).

⁴Sz. Csonka, A. Halbritter, and G. Mihály, *Phys. Rev. B* **73**, 075405 (2006).

⁵Sz. Csonka, A. Halbritter, G. Mihály, E. Jurdik, O. I. Shklyarevskii, S. Speller, and H. van Kempen, *Phys. Rev. Lett.* **90**, 116803 (2003).

⁶Sz. Csonka, A. Halbritter, G. Mihály, O. I. Shklyarevskii, S. Speller, and H. van Kempen, *Phys. Rev. Lett.* **93**, 016802 (2004).

⁷D. Djukic, K. S. Thygesen, C. Untiedt, R. H. M. Smit, K. W. Jacobsen, J. M. van Ruitenbeek, *Phys. Rev. B* **71**, 161402(R) (2005).

⁸A. Halbritter, P. Makk, Sz. Csonka, and G. Mihály, *Phys. Rev. B* **77**, 075402 (2008).

⁹Note that at 4.2 K Nb and Pb are superconducting and so the superconducting excess current modifies the measurement of the conductance, $G=I/U$. However, we have found that this effect is

- hardly noticeable on the rather smooth histograms, and similar histograms were measured at higher bias voltage (30–40 mV) or at higher temperature ($T=10$ K) in the normal state.
- ¹⁰W. H. A. Thijssen, D. Djukic, A. F. Otte, R. H. Bremmer, and J. M. van Ruitenbeek, *Phys. Rev. Lett.* **97**, 226806 (2006).
- ¹¹D. den Boer, O. I. Shklyarevskii, J. A. A. W. Elemans, and S. Speller, *J. Phys.: Conf. Ser.* **61**, 239 (2007).
- ¹²H. E. van den Brom and J. M. van Ruitenbeek, *Phys. Rev. Lett.* **82**, 1526 (1999).
- ¹³B. Ludoph, M. H. Devoret, D. Esteve, C. Urbina, and J. M. van Ruitenbeek, *Phys. Rev. Lett.* **82**, 1530 (1999).
- ¹⁴E. Scheer, N. Agrait, J. C. Cuevas, A. Levy Yeyati, B. Ludoph, A. Martín-Rodero, G. Rubio Bollinger, J. M. van Ruitenbeek, and C. Urbina, *Nature (London)* **394**, 154 (1998).
- ¹⁵B. Ludoph, N. van der Post, E. N. Bratus, E. V. Bezuglyi, V. S. Shumeiko, G. Wendin, and J. M. van Ruitenbeek, *Phys. Rev. B* **61**, 8561 (2000).
- ¹⁶J. J. Riquelme, L. de la Vega, A. Levy Yeyati, N. Agrait, A. Martín-Rodero, and G. Rubio-Bollinger, *Europhys. Lett.* **70**, 663 (2005).
- ¹⁷A. Marchenkov, Z. Dai, C. Zhang, R. N. Barnett, and U. Landman, *Phys. Rev. Lett.* **98**, 046802 (2007).
- ¹⁸E. Scheer, W. Belzig, Y. Naveh, M. H. Devoret, D. Esteve, and C. Urbina, *Phys. Rev. Lett.* **86**, 284 (2001).
- ¹⁹G. Rubio-Bollinger, C. de las Heras, E. Bascones, N. Agrait, F. Guinea, and S. Vieira, *Phys. Rev. B* **67**, 121407(R) (2003).
- ²⁰A. I. Yanson, G. Rubio Bollinger, H. E. van den Brom, N. Agrait, and J. M. van Ruitenbeek, *Nature (London)* **395**, 783 (1998).